JOURNAL OF BACTERIOLOGY, Feb. 1997, p. 742–753 Vol. 179, No. 3
0021-9193/97/$04.00+0

Importance of Structural Differences between Complementary RNA Molecules to Control of Replication of an IncB Plasmid

I. W. WILSON,† K. R. SIEMERING,‡ J. PRASZKIER, AND A. J. PITTARD*

Department of Microbiology, University of Melbourne, Royal Parade, Parkville, Victoria 3052, Australia

Received 17 July 1996/Accepted 12 November 1996

Replication of the IncB miniplasmid pMU720 is dependent on the expression of *repA*, the gene encoding replication initiator protein RepA. Binding of a small antisense RNA (RNAI) to its complementary target (stem-loop I [SLI]) in the RepA mRNA prevents the participation of SLI in the formation of a pseudoknot that is an enhancer of translation of this mRNA. Thus, RNAI regulates the frequency of replication of pMU720 by controlling the efficiency of translation of the RepA mRNA. Mutational analysis of the two seven-base complementary sequences involved in formation of the pseudoknot showed that only the five central bases of each were critical for the formation of the pseudoknot. Physical analysis of SLI showed that despite the complete complementarity of its sequence to that of RNAI, the structures of the two molecules are different. The most prominent difference between the two structures is the presence of a 4-base internal loop immediately below the hairpin loop of SLI but not that of RNAI. Closure of this internal loop in SLI resulted in a 40-fold reduction in *repA* expression and loss of sensitivity of the residual expression to inhibition by RNAI. By contrast, *repA* expression was largely unaffected by the closure of a lower internal loop whose presence in SLI and RNAI is essential for effective interaction between these two molecules. These results suggest that the interaction of SLI with the distal pseudoknot bases is fundamentally different from the RNAI-SLI binding interaction and that the differences in structure between RNAI and SLI are necessary to allow SLI to be able to efficiently bind RNAI and to participate in pseudoknot formation.

The miniplasmid pMU720 is a low-copy-number plasmid belonging to the incompatibility group B. The basic replicon consists of a 3.25-kb DNA fragment that contains the genetic information required for autonomous replication and copy number control. Replication of pMU720 requires the expression of the *repA* gene, whose product is thought to be essential and rate limiting for initiation of replication. Mutational and computer analyses of the folding of the *repA* mRNA (designated RNAII) indicate that its translation is normally inhibited by the presence of a secondary structure, stem-loop III (SLIII), which sequesters the *repA* translational initiation region (23, 35). It has been established for both pMU720 (23, 35) and its close relative, the $IncI_1$ plasmid ColIb-P9 (1, 2), that expression of *repA* (designated *repZ* in ColIb-P9) requires activation of translation of the *repA* mRNA. This process involves the disruption of SLIII by the prior translation and correct termination of a small leader peptide (designated *repB* in pMU720 and *repY* in ColIb-P9), which enables the formation of a pseudoknot adjacent to the *repA* Shine-Dalgarno (SD) sequence. As first demonstrated in ColIb-P9, the formation of the pseudoknot is essential for the translation of *repA* and involves pairing between complementary sequences in the *repA* mRNA. The proximal pseudoknot sequence lies in the loop of a large secondary structure, stem-loop I (SLI), and the distal pseudoknot sequence lies adjacent to the SD sequence of *repA* (Fig. 1). The pseudoknot, which must be in close proximity to the *repA* SD sequence, has been shown to act as an enhancer of translation of *repA*. Its mode of action is unknown but may involve a direct pseudoknot-ribosome interaction (23, 35).

The activation of *repA* expression is negatively regulated by a small, highly structured antisense RNA, called RNAI. The *rnaI* gene resides in the leader region of *repBA* and is transcribed in the direction opposite to that of RNAII, so that RNAI is fully complementary to a ~70-base region of RNAII. A model for the interaction between RNAI and RNAII has been formulated (27, 28). Hybridization between RNAI and its complementary region in RNAII (SLI) inhibits the activation of *repA* translation primarily by sequestering the proximal bases required for pseudoknot formation. The complex formed between RNAI and RNAII also interferes with the access of ribosomes to the translational initiation region of the leader peptide. However, this effect of RNAI on the translation of the leader peptide has been found to be relatively unimportant for the regulation of *repA* expression (36).

Analysis of the physical structure of RNAI revealed the presence of nonconventional U-U base pairs in its upper stem (27). The complementary region in the target of RNAI, the SLI of RNAII, is predicted to be unpaired because it is known that hydrogen bonding does not occur between consecutive A · A mismatches in partially complementary RNA oligonucleotides (26). Siemering et al. (27) postulated that this difference between the structures of the two molecules may be an essential feature of the copy number control system of pMU720. It was proposed that the more open loop structure of SLI may be necessary to give SLI sufficient flexibility to enable it to participate in the two different, mutually exclusive reactions it is involved in, i.e., an intermolecular interaction with RNAI and an intramolecular interaction to form the pseudoknot. Given that the intermolecular interaction involves two stem-loop structures whereas the intramolecular one involves a hairpin loop and a linear sequence, the binding pathways of the two reactions are likely to be different and the participating RNA molecules may have different structural requirements for optimal reactivity.

In this paper, we describe the secondary structure of SLI and

* Corresponding author. Phone: 61 3 9344 5679. Fax: 61 3 9347 1540. E-mail: aj.pittard@microbiology.unimelb.edu.au.

† Present address: Department of Plant Biology, Carnegie Institution of Washington, Stanford, CA 94305.

‡ Present address: MRC Laboratory of Molecular Biology, Genome Studies Section, Cambridge CB2 2QH, United Kingdom.

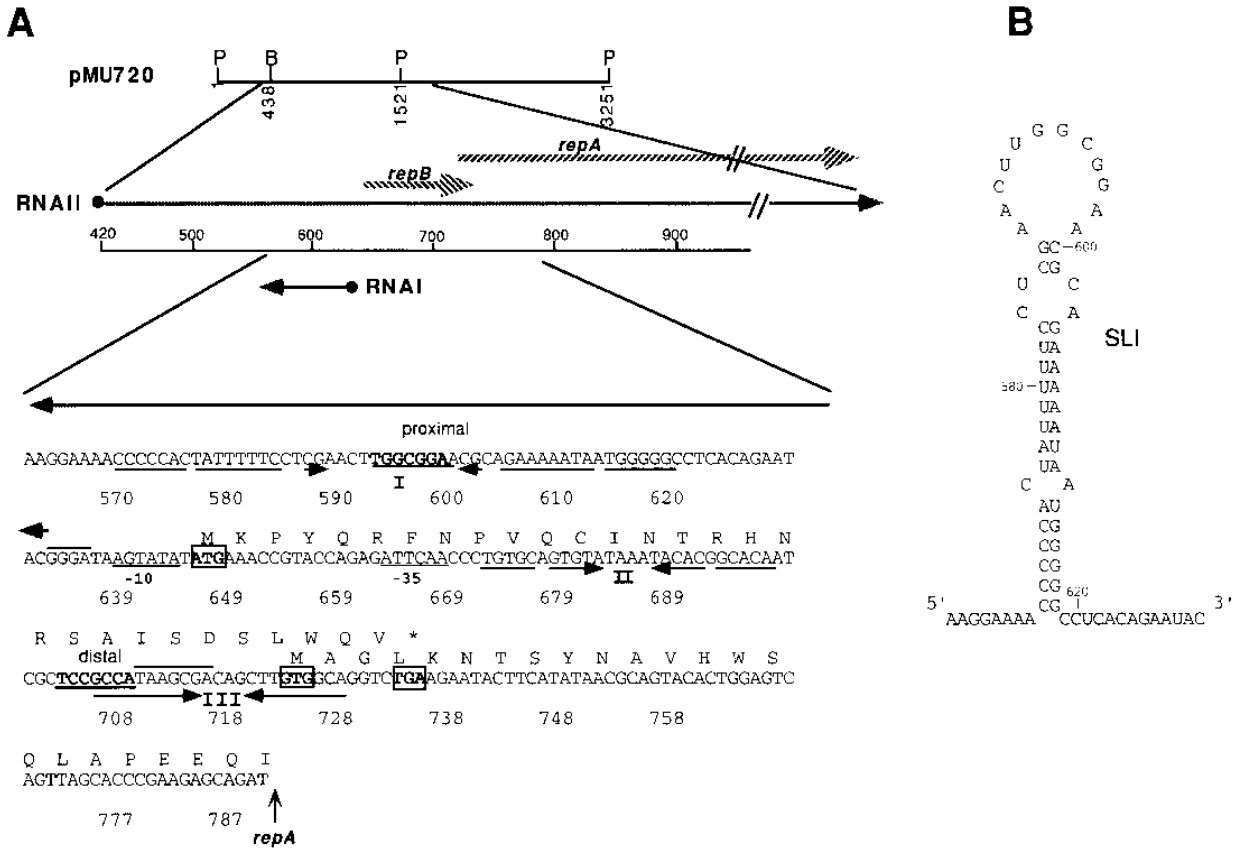

FIG. 1. (A) Replication control region of pMU720. RNAI and RNAII transcripts and the coding regions of the two *rep* genes (hatched arrows) are indicated. The nucleotide sequence between base positions 561 and 789 together with the amino acid sequence of *repB* and the amino-terminal end of *repA* is shown. The initiation and termination codons are boxed, and the putative Shine-Dalgarno sequences of the two genes are overlined. The promoter region of RNAI and the putative stem-loop structures I, II, and III are indicated. The complementary proximal and distal pseudoknot sequences are underlined and shown in boldface. The vertical arrow indicates the 3′ end of the pMU720 fragment inserted into the fusion vectors. Abbreviations: P, *Pst*I; B, *Bam*HI. (B) Predicted secondary structure of SLI of RNAII.

the use of site-directed mutagenesis to evaluate the importance of nucleotides in its hairpin loop and upper stem to the pseudoknot-induced translational enhancement of *repA* expression. The data confirm the presence of an internal loop immediately below the hairpin loop of SLI and show that it is essential for both the intermolecular and the intramolecular interaction.

MATERIALS AND METHODS

Bacterial strains, plasmids, and phages. The strains of *Escherichia coli* K-12 used in this study are given below. JM101 [Δ(*lac-proAB*) *supE thi* F′(*traD36 proA*$^+$*B*$^+$ *lacI*^{q}*ZΔM15*)] (15) was used for cloning and propagating M13 derivatives. SDM [*hsdR17 mcrAB recA1 supE44* Tet^r Δ(*lac-proAB*) F′(*traD36 proA*$^+$*B*$^+$ *lacI*^{q}*ZΔM15*)] was used to grow M13 derivatives which had undergone mutagenesis as described by Vandeyar et al. (32). JP3923 (*thr-1 leuB6 thi-1 lacZΔM15 lacY1 gal-351 supE44 tonA21 hsdR4 gyrA379 rpsL743 recA56 srl-1300*::*Tn10 aroL513*) was used for all β-galactosidase assays with translational and transcriptional *lacZ* fusions. JP8042 (Δ*lacU169 tyrR366 recA56*) was used for all β-galactosidase assays used for copy number determinations (38).

Bacteriophage vectors used to clone fragments for DNA sequencing and mutagenesis were M13tg130 and M13tg131 (14) and their derivatives, mpMU583 and mpMU556. These M13 derivatives contain an *Eco*RI-*Bgl*II insert encompassing nucleotides (nt) 1 to 789 of pMU720. They differ only in that mpMU583 carries the RNAI.3 mutation in the −10 region of the *rnaI* promoter. The plasmids and phages used are described in Table 1.

Media, enzymes, and chemicals. The minimal medium used was half-strength buffer 56 (17) supplemented with 0.2% glucose, thiamine (10 μg/ml), and necessary growth factors. Enzymes and chemicals of a suitable grade were purchased commercially and not purified further. [^{35}S]dATPaS (1,000 to 1,500 Ci/mmol) for use in sequencing and [γ-^{32}P]GTP (6,000 Ci/mmol) for 5′-end labelling of RNA were obtained from NEN Research Products. Ampicillin was used at a final concentration of 50 μg/ml, trimethoprim was used at 10 μg/ml, isopropyl-β-D-thiogalactopyranoside (IPTG) was used at 1 mM, and 5-bromo-4-chloro-3-indolyl-D-galactopyranoside (X-Gal) was used at 25 μg/ml.

Recombinant DNA techniques. Plasmid and bacteriophage DNAs were isolated and manipulated as described by Sambrook et al. (24). The method used for DNA sequencing was that described by Sanger et al. (25), except that T7 DNA polymerase was used instead of the Klenow fragment and terminated chains were uniformly labelled with [^{35}S]dATPaS. Oligonucleotide-directed in vitro mutagenesis reactions were performed on single-stranded M13 templates with a kit from United States Biochemical Corp. Oligonucleotides were synthesized with the Gene Assembler Plus (Pharmacia LKB Biotechnology). DNA sequencing was used to screen for and confirm the presence of mutations.

Generation of chimeric SLI structures. The SLI-like regions from $IncI_1$ (pMU605), IncIγ (pMU1530), IncK (pMU2209), IncZ (pMU2200), IncL/M (pMU604), and FII (pMU600) plasmids were amplified by PCR with forward and reverse primers containing *Xba*I and *Apa*I linkers, respectively, at their 5′ ends. These DNA fragments were then inserted into the *Xba*I-*Apa*I sites of mpMU584 and mpMU201 and sequenced. Clones carrying error-free inserts were used as the source of DNA for the construction of derivatives of pMU1550, pMU1551, and pBR322.

Construction of the *lacZ* fusion plasmids. The construction of *repA-lacZ* translational (pMU1550) and transcriptional (pMU1551) plasmids has been described previously (23). Plasmid pMU1550 is pMU525 (21) carrying nt 1 to 789 of pMU720, which fuses codon 23 of *repA* with codon 8 of *lacZ*. β-Galactosidase expression in pMU1550 is therefore dependent on transcription from the RNAII promoter and translational initiation from *repA*. The transcriptional *lacZ* fusion vector pMU1551 was constructed from pMU2385 (23) by the insertion of nt 1 to 789 of pMU720, so that β-galactosidase expression is dependent on transcription from the RNAII promoter and translational initiation from *galK*. Mutant derivatives of these *repA-lacZ* fusions were constructed by replacing the wild-type 789-bp *Eco*RI-*Bgl*II fragment of pMU1550 or pMU1551 with the 789-bp *Eco*RI-*Bgl*II fragment containing the mutation to be tested.

Construction of pBR322 derivatives. The construction of pMU617 and pMU662 has been described previously (21). pMU617, which is pBR322 carrying

TABLE 1. Plasmids and phages

Plasmid or phage	Relevant characteristics[a]	Source or reference
Plasmids		
pBR322	pMB1 derivative; Ap Tc	29
pAM34	pBR322 derivative in which the preprimer RNA is expressed from *lacZpo*; *lacI*^{q} Ap Sp	8
pMU720	Miniplasmid; Gal IncB	5
pMU604	Miniplasmid; Gal IncL/M	7
pMU605	Miniplasmid; Gal IncI_1	7
pMU1530	Miniplasmid; Gal IncIγ	18
pMU600	Miniplasmid; Gal IncFII	7
pMU2200	Miniplasmid; Gal IncZ	22
pMU2209	Miniplasmid; Gal IncK	22
pMU2441	pGEM-3Z derivative carrying nt 552 to 639 of pMU720	28
pMU4365	Dual origin plasmid derived from pAM34 and pMU720 for use in copy number determinations	36
pMU525	Low-copy-number translational-fusion vector; *lac′ZYA′* Tp IncW	21
pMU2385	Low-copy-number transcriptional-fusion vector, *galK′-lac′Z* Tp IncW	23
pMU1550	*repA-lacZ* translational fusion carrying nt 1 to 789 of pMU720; Tp IncW IncB	23
pMU1551	*repA-lacZ* transcriptional fusion carrying nt 1 to 789 of pMU720; Tp IncW IncB	23
pMU2371	*repA-lacZ* translational fusion carrying nt 1 to 789 of pMU720 with RNAI.3 mutation; Tp IncW	36
pMU2372	*repA-lacZ* transcriptional fusion carrying nt 1 to 789 of pMU720 with RNAI.3 mutation; Tp IncW	36
pMU617	pBR322 carrying nt 438 to 718 of pMU720; Ap IncB	21
pMU662	pBR322 carrying nt 1 to 637 of pMU720	21
pMU4565-4566, pMU4572-4573, pMU4578-4579	pBR322 derivatives carrying the *Xba*I-*Bgl*II fragments containing the chimeric *rnaI* genes excised from derivatives of mpMU201; Ap and IncIγ, -FII, -K, -Z, -L/M, or -I_1, respectively	This study
Phages		
mpMU556	M13tg130 derivative carrying nt 1 to 789 of pMU720 on an *Eco*RI-*Bgl*II fragment	36
mpMU583	mpMU556 carrying the RNAI.3 mutation	This study
mpMU201	mpMU556 carrying the SLI.3 mutation	This study
mpMU584	mpMU583 carrying the SLI.3 mutation	This study

[a] Abbreviations: Ap, ampicillin resistance; Sp, spectinomycin resistance; Tc, tetracycline resistance; Tp, trimethoprim resistance; Gal, ability to promote fermentation of galactose. Mutations introduced into the *repA-lacZ* fusion plasmids, pMU4365 and pBR322, and M13 derivatives are described in Results.

nt 438 to 718 of pMU720 (Fig. 1), expresses RNAI (but not RNAII) from its own promoter and is used to deliver extra copies of RNAI. pMU662 is pBR322 carrying the first 637 nt of pMU720 (Fig. 1) and therefore expresses the leader region of RNAII, including SLI, which is the target for RNAI, but does not express RNAI. This plasmid is used to titrate out RNAI molecules synthesized by other plasmids. Plasmids pMU4565-4566, pMU4572-4573, and pMU4578-4579 were constructed by excising the *Bgl*II-*Xba*I fragment containing the chimeric *rnaI* gene from the appropriate mpMU201 derivative and inserting it into the *Bam*HI-*Nhe*I site of pBR322. None of the pBR322 derivatives carries *lacZ*.

Construction of plasmids for use in copy number determinations. Plasmids for use in copy number determinations were derived from pMU4365 by replacing the wild-type 789-bp *Eco*RI-*Bgl*II fragment of pMU4365 with the 789-bp *Eco*RI-*Bgl*II fragment containing the mutation to be tested. The chimeric plasmid pMU4365 (36) contains both the IncB replicon and the replicon from pAM34 (8). The latter is a modified pMB1 replicon in which the essential preprimer RNA is transcribed from the *lacZ* promoter operator. Since pMU4365 also contains the *lacI*^{q} gene, replication of the pAM34 replicon is dependent on the presence of IPTG. Thus, in the absence of IPTG, replication of pMU4365 is reliant on the IncB replicon. As well as allowing the rescue of mutations deficient in IncB plasmid replication, this plasmid also permits determination of relative copy numbers by making use of a *lacZ* reporter gene, which is expressed constitutively from the *tyrP* promoter in a *tyrR* strain (JP8042).

Measurement of β-galactosidase activity. β-Galactosidase activities of mid-log-phase cultures were assayed as described by Miller (16). Each sample was done in duplicate, and each assay was performed at least three times.

Prediction of RNA secondary structures. The computer programs of Zuker and his colleagues (12, 13, 39) were used to predict RNA secondary structures.

Construction of the template for in vitro transcription of $RNAII_{107}$. Plasmid pMU2441, used as the template for transcription of $RNAII_{107}$, was constructed by inserting a PCR-generated *Eco*RI-*Bgl*II fragment containing nt 552 to 639 of pMU720 into an *Eco*RI- and *Bam*HI-cleaved T7 transcription vector, pGEM-3Z. Synthesis and sequence analysis of the *Eco*RI-*Bgl*II PCR fragment were performed essentially as described previously (23).

Preparation of $RNAII_{107}$. Transcripts radiolabelled at their 5′ ends were synthesized in vitro from *Xba*I-linearized pMU2441 with T7 RNA polymerase. A standard 100-μl transcription mixture contained 40 mM Tris-HCl (pH 7.5), 6 mM $MgCl_2$, 2 mM spermidine, 10 mM NaCl, 10 mm dithiothreitol, 100 μM GTP, 500 μM each ATP, CTP, and UTP, and 200 μCi of [γ-^{32}P]GTP, 2 U of RNasin, 14 U of T7 RNA polymerase, and 6 to 8 μg of *Xba*I-linearized pMU2441. After incubation for 90 min at 37°C, RNA was isolated, purified, and renatured as described previously (19).

Analysis of secondary structure of $RNAII_{107}$. Typically, 1,000 Cerenkov cpm of 5′-labelled $RNAII_{107}$ was partially digested for 5 min at 37°C with either T1, T2, A, or V1 RNase as described by Wagner and Nordström (33). The amounts of each RNase used in a standard partial digest were 1.7×10^{-2} U (T1), 5.0×10^{-2} U (T2), 1.8×10^{-6} U (A), and 5.0×10^{-2} U (V1). Alkaline hydrolysis ladders were prepared as described previously (33). Partial T1 digestion under denaturing conditions was carried out as described by Wrede et al. (37). Samples were heated to 100°C for 3 min prior to electrophoresis on 20% polyacrylamide gels containing 7 M urea. Autoradiography was at −70°C for 48 h with Kodak X-AR 5 film with intensifying screens.

RESULTS

Secondary structure of SLI. Computer modeling of the secondary structure of SLI predicted the formation of a stem containing a 4-base interior loop, topped by a 12-base hairpin loop (Fig. 1B). This structure is significantly different from that elucidated for the antisense RNAI, the molecule complementary to SLI, which was found to possess a long stem containing a 2-base interior loop and nonconventional U-U base pairs just below a 6-base hairpin loop (27). To determine whether the hairpin loop regions of RNAI and SLI are indeed different from each other, physical analysis of the structure of SLI was performed by using, for convenience, a truncated RNAII transcript comprising SLI plus flanking sequences. As described in Materials and Methods a 5′-end-labelled RNA transcript consisting of nt 552 to 639 of pMU720 ($RNAII_{107}$) was produced in vitro, purified, and partially digested with structure-probing RNases T1 (specific for G residues in a single-stranded region), T2 (single strand specific), and V1 (double strand specific). Cleavage products were analyzed by electrophoresis on 20% polyacrylamide gels (Fig. 2).

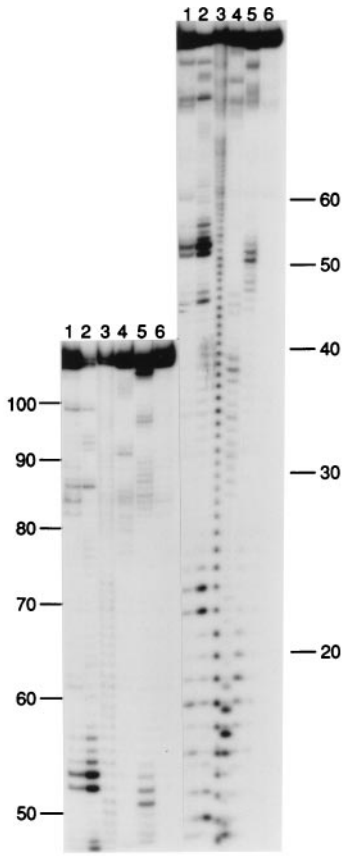

FIG. 2. Probing of the secondary structure of $RNAII_{107}$ by partial RNase digestion. 5′-end-labelled $RNAII_{107}$ was prepared and partially cleaved as described in Materials and Methods. Electrophoresis was on a 20% polyacrylamide gel with sequential loading of samples (left and right sections of the gel are shown). The numbers on the right and left indicate the positions of the cleavage sites in $RNAII_{107}$. Lanes: 1, RNase T_1 digestion; 2, RNase T_1 digestion under denaturing conditions; 3, alkaline hydrolysis ladder; 4, RNase VI digestion; 5, RNase T_2 digestion; 6, no enzyme. All bands ran as doublets, presumably due to initiation of transcription at heterogeneous points or slippage early in synthesis by T7 RNA polymerase during in vitro transcription. In all cases, the strongest lower band of each doublet was used to determine the cleavage site. The numbers indicate the nucleotide positions in $RNAII_{107}$ relative to the 5′ end of the molecule.

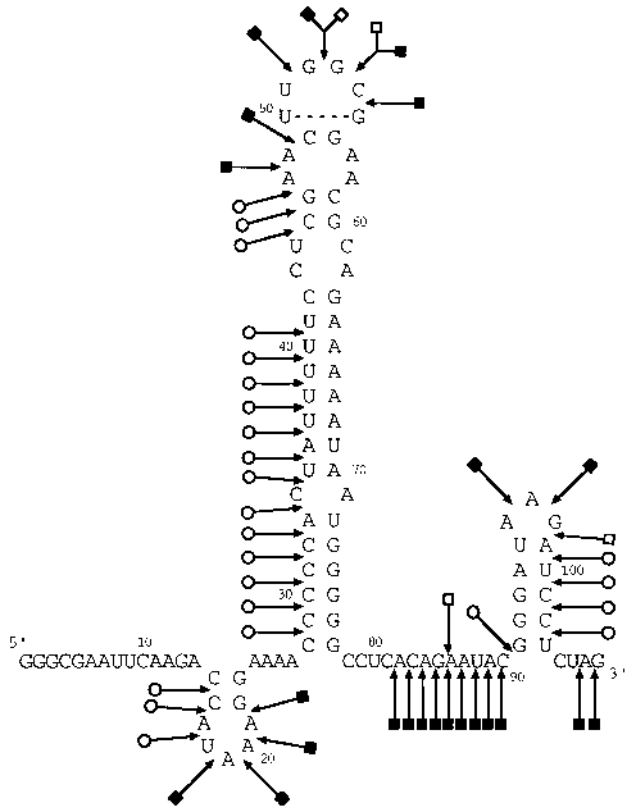

FIG. 3. Structure proposed for SLI and summary of partial digestion data. The numbers indicate the nucleotide positions in $RNAII_{107}$ relative to the 5′ end of the molecule. The arrows indicate the sites of cleavage by the following RNases: RNase T_2 (■), RNase A (□), RNase T_1 (●), and RNase V1 (○).

When 5′-end-labelled $RNAII_{107}$ was probed with the RNase V1, extensive cleavage was observed on the 5′ side of the predicted stem of SLI, at positions 28 to 40 and 44 to 46 (Fig. 2). The stems of the small stem-loop structures predicted to exist 5′ and 3′ to SLI were also found to be susceptible to cleavage by RNase V1. The reason why no cutting was observed on the 3′ side of the stem of SLI is unclear. However, RNase V1 cleaved the antisense RNAs of the IncB and IncFII plasmids also predominantly on the 5′ side of the stems of these molecules (27, 33). Digestion of $RNAII_{107}$ with single-strand-specific RNases, T1 and T2, resulted in cleavages at residues in the predicted hairpin loop and in the 3′ single-stranded tail of SLI. Cutting was observed at positions 47, 48, and 51 to 54 in the hairpin loop and at positions 81 to 89 in the 3′ tail. Cleavages were also observed in the predicted loops of the two smaller stem-loop structures. A summary of these cleavage data and the structure proposed for SLI are presented in Fig. 3. As was the case with elucidation of the secondary structure of RNAI (27), the results generally support the computer-generated prediction of secondary structure (Fig. 1B). Extensive digestion by RNase V1 confirmed the presence of the stem of SLI. However, as was found also on analyzing RNAI, digestions carried out with the single-strand-specific RNases indicate that the hairpin loop of SLI comprises fewer than the predicted 12 nt. The RNases T1 and T2 clearly cut at positions 51 to 54, indicating that SLI contains a 4-base loop comprising these nucleotides. The observation that RNase T1 did not cut at either the base guanine at position 55 (G55) or G56 and that RNase T2 did not cut at G55, G56, C49, or U50 suggests that this 4-base loop is closed by C-G pairing between C49 and G56 and U-G pairing between U50 and G55. However, considering that U-G pairing is not strong and that a 6-base hairpin loop is energetically more favorable than a 4-base loop (30), it is probable that the 4-base loop closed by pairing between U50 and G55 is in equilibrium with a 6-base loop closed by pairing between C49 and G56. The observation that digestion by RNase T2 yielded cleavages at A47 and A48 in the lower loop suggests that, whereas U-U pairing is proposed to exist in the upper stem of RNAI (see Fig. 4), similar A-A pairing does not occur in the comparable region of $RNAII_{107}$. This conclusion is supported by the finding that there is no hydrogen bonding between A-A mismatches in partially complementary RNA oligonucleotides that contain consecutive A-A mismatches (26).

These data support the prediction that SLI and RNAI form structures that are significantly different from each other. Thus, RNAI contains nonconventional U-U base pairs immediately below its 6-base loop, whereas the presence of A-A mismatches in the comparable region of SLI results in the formation of an internal loop (Fig. 4). The structure of SLI also

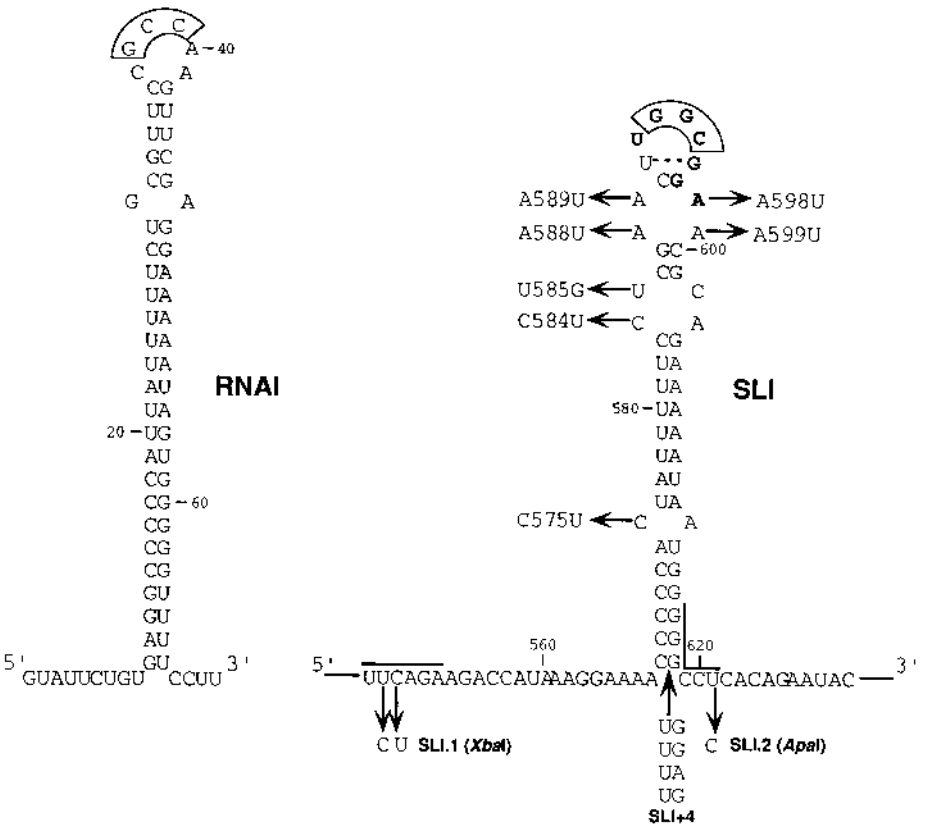

FIG. 4. Secondary structures of RNAI and SLI, as determined by structural analyses, showing the base substitutions used to determine the importance of the structure of SLI for the formation of the pseudoknot as well as mutations introduced into the *repA* fragment to allow the substitution of the IncB SLI with the SLI-like structures from other plasmids. Proximal pseudoknot bases are in boldface. The site and base changes of the mutations introduced are indicated. The nucleotide numbers indicated for RNAI are counted from the 5′ end of the molecule, whereas for SLI, the nucleotide numbers are those of pMU720. The three bases which are critical for RNAI-SLI binding are enclosed in a box.

differs from that of RNAI in that its stem is shorter by 4 bp and contains a 4-base lower internal loop compared with the 2-base internal loop of RNAI. Finally, the hairpin loop of SLI is proposed to exist in an equilibrium between a 4- and 6-base form, whereas RNAI clearly possesses a 6-base loop.

Importance of individual bases for pseudoknot formation. Although the importance of base pairing between the proximal and distal pseudoknot bases to the expression of *repA* has been confirmed in pMU720 (23, 35), the extent to which individual bases contribute to the pseudoknot-induced translational enhancement of *repA* has not been determined. Since the translation of *repA* has been shown to be almost totally dependent on base pairing between proximal and distal pseudoknot bases (23, 27, 35, 36), any reduction in the ability of the pseudoknot to form or function correctly should lead to a corresponding reduction in the expression of *repA*. Therefore, to systematically analyze the relative importance of individual pseudoknot bases, site-directed mutagenesis was used to substitute each of the proximal and distal bases to prevent base pairing at that position (Fig. 5). The effects of these mutations on the expression of *repA* were measured with low-copy-number plasmids (approximately 1 to 2 copies per chromosome) carrying translational *repA-lacZ* fusions in which codon 23 of *repA* was fused in phase with codon 8 of *lacZ*. Although RNAII is expressed constitutively (21), the DNA fragment used to construct the *repA-lacZ* translational fusion was also introduced into a *lacZ* transcriptional fusion pMU2385 (23) to confirm that the mutations had no effect on transcription.

Since SLI and RNAI are encoded within the same piece of DNA, any mutation introduced into the proximal pseudoknot bases located in SLI will also result in a change to RNAI and may affect the interaction between RNAI and SLI by altering

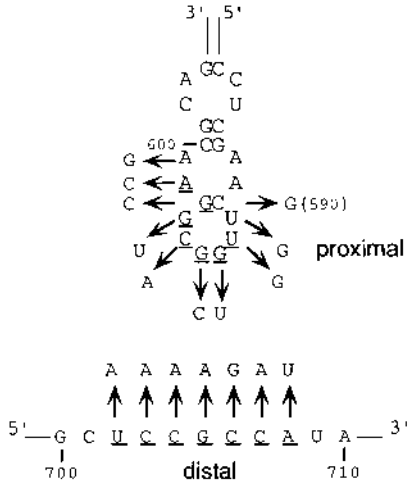

FIG. 5. Diagrammatic representation of the base substitutions used to determine the importance of the individual distal and proximal pseudoknot bases for the formation of the pseudoknot. Complementary pseudoknot bases are underlined. The site and base changes of the mutations introduced are indicated.

TABLE 2. Effects of mutations which alter the proximal pseudoknot sequence on the expression of β-galactosidase from *repA-lacZ* fusions carrying the RNAI.3 mutation

Mutation[a]	β-Galactosidase activity (U) from[b]:	
	Translational fusion	Transcriptional fusion
None	4,129	991
C590G	1,479	867
U592G	946	1,125
G593U	11	968
G594C	10	944
C595A	12	1,014
G596U	45	1,036
G597C	87	1,250
A598C	4,469	2,223
U591G	3,319	960
A599G	4,416	1,252

[a] All the mutations were introduced into a *repA-lacZ* fusion carrying the RNAI.3 mutation.

[b] β-Galactosidase activities from the *repA-lacZ* fusion were measured by the method of Miller (16), and the values shown are the averages of at least three independent determinations. To allow comparison with previous assays, all β-galactosidase activities were measured for cells which contained the plasmid pBR322 in *trans* to the *lacZ* fusion plasmid. The parental plasmid pMU525 or pMU2385 with pBR322 in *trans* produced <1.0 U of β-galactosidase activity.

TABLE 3. Effects of mutations in the distal pseudoknot sequence on expression of β-galactosidase from *repA-lacZ* fusions, and IncB plasmid replication

Mutation	β-Galactosidase activity (U) from[a]:				Relative plasmid copy no.[b]
	Translational fusion with:			Transcriptional fusion with pBR322	
	pBR322	pMU617 (RNAI)	pMU662 (target)		
None	124	0.1	1,283	113	1.0
T702A	127	0.5	731	245	0.9
C703A	16.5	0.5	79	153	0.2
C704A[c]	2.0	<0.1	18	155	NV[d]
G705A	6.1	0.2	28	116	NV
C706G[c]	17	3.4	41	34	0.4
C707A	7.0	5.0	14	39	0.4
A708T	74	0.4	481	123	1.2

[a] β-Galactosidase activities from *repA-lacZ* fusion with coresident plasmid present in *trans* were measured by the method of Miller (16), and the values shown are the averages of at least three independent determinations. The vector (pBR322) or its derivatives were present in *trans*. pMU617 (RNAI) carries nt 438 to 718 of pMU720 and therefore expresses RNAI but not RNAII (21). pMU662 (target) carries nt 1 to 637 of pMU720 (21) and thus expresses the leader sequence of RNAII (SLI), which is complementary to RNAI, but does not express RNAI. These plasmids do not carry *lacZ*. The parental plasmid pMU525 or pMU2385 with pBR322 in *trans* produced <1.0 U of β-galactosidase activity.

[b] Copy number determinations were carried out with strain JP8042 grown in minimal medium containing glucose as the carbon source and ampicillin. β-Galactosidase activities obtained with mutant derivatives of pMU4365 were normalized to the activities obtained with pMU4365.

[c] The RNAI and target RNA added in *trans* to fusions with substitutions at positions 594 and 596 carried the appropriate mutations to retain full complementarity with the RNAI and RNAII targets.

[d] NV, replication of the pMU4365 derivative could not be maintained without IPTG.

the structure of RNAI or changing the specificity of pairing between the two molecules, thereby altering the expression of *repA*. To avoid this complication, all substitutions in the proximal pseudoknot sequence were introduced into a *repA-lacZ* translational fusion containing the RNAI.3 mutation, which changes the −10 sequence of the *rnaI* promoter from TAT ACT to TGTGCG, and has been shown to eliminate the expression of *rnaI* (36). Therefore, in this experimental scheme, the expression of *repA-lacZ* is dependent only on the efficiency of pseudoknot formation and its effectiveness as an enhancer of translation of the *repA* mRNA. Since the introduction of the RNAI.3 mutation does not allow the isolation of reconstituted IncB replicons (34), the effect on copy number of substitutions in the proximal sequence could not be assessed.

From Table 2, it can be seen that mutations in five of the seven proximal bases (nt 593 to 597) significantly reduced *repA* expression (47- to 430-fold reductions), with substitutions at positions 593, 594, and 595 resulting in the greatest reductions. Transcriptional controls show that the results obtained must be due to translational effects. By contrast, changes to base U592 (U-to-G change at position 592 [U592G]) resulted in only a fourfold reduction, whereas A598C increased β-galactosidase expression from both the *repA-lacZ* translational and transcriptional fusions. The loop size of RNA molecules has been shown to be important for RNA-RNA interactions (10), with loop sizes of 7 and 6 bases thought to favor highly specific and rapid recognition of a target RNA sequence (9). Because the mutation G597C not only disrupts the complementarity of the pseudoknot sequences but is also predicted to open the loop domain of SLI to create a 12-base loop (Fig. 5), the effect of increasing the size of the loop of SLI without changing pseudoknot bases was tested. Enlarging the loop of SLI to 12 bases by the introduction of the C590G mutation (Fig. 5) reduced β-galactosidase expression from the *repA-lacZ* translational fusion threefold without significantly affecting expression from the equivalent transcriptional fusion (Table 2). Thus, although the creation of a 12-base loop does impair the pseudoknot-dependent enhancement of translation, this effect is far less significant than that conferred by the G597C mutation. These data clearly indicate that whereas bases at positions 593 to 597 are crucial for the formation or function of the pseudoknot, those at positions 592 and 598 are not.

To confirm this conclusion, we examined the effects of substituting bases in the distal pseudoknot sequence. Since these mutations do not affect SLI or RNAI, they were introduced into a wild-type *repA* fragment. To evaluate the effect of the mutations on the regulation of *repA* by RNAI, assays were performed in the presence of multicopy plasmids (20 to 30 copies per chromosome) carrying either the *rnaI* gene (producing saturating levels of RNAI, resulting in maximal inhibition) or the gene for the RNA complementary to RNAI (i.e., target RNA to titrate out RNAI, resulting in a fully derepressed state). These mutations were also inserted into the IncB replicon of the chimeric plasmid pMU4365 (36) to examine their effect on the replication of the IncB plasmid.

From Table 3, it can be seen that substituting bases at positions 702 and 708 had little effect on the expression of *repA* and the copy number of the IncB plasmid, confirming that the A598-U702 and U592-A708 base pairings are relatively unimportant for the formation of the pseudoknot. Nevertheless, since mutations in T702 and A708 did lead to two- to threefold decreases in the fully derepressed expression of *repA* (pMU662 in *trans*), they do make some contribution to the formation or stability of the pseudoknot. By contrast, substituting bases at positions 703 to 707 had a drastic effect on the expression of *repA* and the copy number of the IncB plasmid, reducing the expression of β-galactosidase from *repA-lacZ* translational fusions from 7- to 62-fold under normal conditions and from 16- to 92-fold when the expression of *repA* was fully derepressed (pMU662 in *trans*). The highest relative copy number achieved by an IncB plasmid carrying a mutation at one of these locations was 0.4, with the C704A and G705A mutations both

resulting in plasmids that were unable to replicate. Although these mutations affected the expression from the *repA-lacZ* transcriptional fusion (especially C706G and C707A), the translational effect was much more profound than the transcriptional one. Assessing the actual relative importance of these five bases was made difficult by the observation that substitution of either C706 or C707 resulted in large levels of RNAI-insensitive expression, suggesting that these mutations also lead to disruptions of SLIII, and therefore allow some independent expression of *repA*. The relatively large RNAI-insensitive expression from these mutants may also account for the higher-than-expected copy number of the IncB plasmids carrying these mutations.

Thus, data obtained with both the distal and proximal mutations indicate that only five of the seven pseudoknot base pairs are important for the formation and function of the pseudoknot and that the other two base pairs play only a minor role. Bases 593, 594, and 595, which appear to be the most important of the proximal bases for the pseudoknot, have also been found to be essential for the initial RNAI-SLI interaction (27, 28), supporting the hypothesis that RNAI controls the expression of *repA* directly through the inhibition of the formation of the pseudoknot.

Effect of increasing the complementarity of the pseudoknot sequences on the expression of *repA*. Siemering et al. (27) suggested that increasing the length of complementarity between the proximal and distal bases may increase the efficiency of pseudoknot formation and lead to greater expression of *repA*. This notion was put forward to explain the unexpectedly high copy number of some IncB plasmids that contained mutations in SLI which were thought to be unimportant for the RNAI-RNAII interaction but had the potential to extend the complementarity of the pseudoknot sequences. To test this theory, bases flanking the proximal sequence in SLI were substituted (U591G and A599G) to make it possible for them to pair with bases flanking the distal pseudoknot sequence (Fig. 5). Once again, to avoid possible complications caused by effects of these base substitutions on the binding affinities between RNAI and SLI, the mutations were introduced into *repA* fragment carrying the RNAI.3 mutation.

Extending the complementarity of the pseudoknot sequences by one extra base 5′ to the proximal sequence (U591G) resulted in a slight decrease in the expression of *repA*, whereas extending the complementarity 3′ of the proximal sequence (allowing pairing between G599 and C701) slightly increased β-galactosidase expression from both the *repA-lacZ* translational and transcriptional fusions (Table 2). Thus, increasing the length of sequence complementarity between the proximal and distal bases to 8 bp does not significantly enhance the translation of the *repA* mRNA.

Effect of altering the structure of SLI on the formation of the pseudoknot. The structural analysis of SLI presented above confirmed the major differences between the structures of RNAI and SLI. It has been hypothesized that these differences may facilitate the different functions of the two RNA molecules in that RNAI is required to bind only to SLI, whereas SLI is bifunctional and must not only be able to interact with RNAI but must also be able to form a pseudoknot (27). To better understand the structural requirements for the formation and function of pseudoknot, site-directed mutagenesis was performed to specifically alter the structure of SLI, without affecting the proximal pseudoknot bases (Fig. 4). To examine the effect of these mutations on the ability of SLI to bind RNAI, β-galactosidase assays were also performed in the presence of excess wild-type RNAI (pMU617 in *trans*) (Table 4). To limit the effects of these mutations to pseudoknot only, the mutations were again introduced into the *repA* fragment carrying the RNAI.3 mutation.

TABLE 4. Effects of mutations which alter the structure of SLI on the expression of β-galactosidase from *repA-lacZ* fusions carrying the RNAI.3 mutation

Mutation[a]	β-Galactosidase activity (U) from[b]:		
	Translational fusion with:		Transcriptional fusion with pBR322
	pBR322	pMU617 (RNAI)	
None	4,129	0.2	991
A588U	4,340	1.0	717
A589U	1,779	1.3	679
A588U-A589U	128	56	783
A588U-A589U-A598U-A599U	103	42	1,449
C584U	5,045	1.2	878
U585G	3,158	336	1,226
C584U-U585G	2,753	434	1,120
C575U	3,973	0.1	904
SLI+4	2,543	1.0	900

[a] See Table 2, footnote *a*.
[b] See Table 3, footnote *a*.

(i) Mutations in upper interior loop. The major difference between RNAI and SLI lies in the region below the loop domain. SLI contains an upper interior loop consisting of A-A mismatches comprising the nucleotides A588, A589, A598, and A599, whereas the equivalent region of RNAI contains consecutive U-U base pairs. The predicted partial closure of the upper interior loop by the introduction of the A588U mutation (allowing pairing between U588 and A599) had little effect on the expression of *repA*, and the predicted partial closure of this loop with A589U (Fig. 4) decreased *repA* expression by approximately twofold (Table 4). The expression of *repA* in both these mutants was still subject to control by wild-type RNAI. Combining the two mutations, which is predicted to close this interior loop, resulted in a 32-fold decrease in *repA* expression, with the residual expression being largely insensitive to excess wild-type RNAI added in *trans* (Table 5). Similarily, replacing the interior loop of SLI with the weakly stabilized U-U pairing that exists in RNAI (A588U-A589U-A598U-A599U mutation) also severely reduced the translation of *repA* (by 40-fold) and its sensitivity to control by RNAI. Although the introduction of the A588U-A589U-A598U-A599U mutation also reduces the complementarity of the proximal pseudoknot sequences at position 598, this position was shown to be unimportant for the formation or function of the pseudoknot (Table 2). The β-galactosidase expression from the *repA-lacZ* transcriptional fusions showed that the effects obtained must be translational in origin.

These data indicate that both the structure of SLI and the complementarity of its proximal pseudoknot bases to the distal ones are extremely important for its ability to participate in the formation of the pseudoknot. In particular, the presence of the upper interior loop in SLI is important for the correct formation or efficient function of pseudoknot. The observation that the U-U pairing that occurs in RNAI leads to severe reduction in *repA* expression when introduced into the equivalent region of SLI supports the notion that the different structure of the two RNA molecules is necessary for their different functions.

(ii) Mutations in lower interior loop and stem of SLI. Siemering et al. (27, 28) demonstrated that in pMU720 the 2-base internal loop of RNAI (G30-A47) (Fig. 4) is essential for the RNAI-SLI interaction since it allows intrastrand melting and interstrand pairing between the two molecules follow-

ing the initial contact at their hairpin loops. To investigate whether the presence of an equivalent internal loop in SLI is required for the effective formation of the pseudoknot, C584U and U585G mutations (Fig. 4) were used to alter this structure and β-galactosidase assays were performed to assess the effect of these changes on expression of *repA-lacZ*. The data in Table 4 demonstrate that closure of the lower portion of the loop by the introduction of the C584U mutation (which makes SLI similar in structure in this region to RNAI) resulted in a slight increase in *repA-lacZ* expression (from 4,130 to 5,045 U), without affecting the ability of SLI to bind RNAI. Closure of the upper portion of the interior loop with the U585G mutation slightly lowered the expression of *repA*, despite an increased expression from the equivalent transcriptional fusion. As predicted from the work of Siemering et al. (27, 28), this mutation also greatly reduced the ability of the wild-type RNAI to control the expression of *repA*. The effect of combining the two mutations (C584U and U585G), which is predicted to completely close the lower interior loop, was essentially the same as that obtained with U585G alone (Table 4). These data indicate that although the lower interior loop of SLI is essential for the RNA-SLI interaction, it is not required for the formation or function of the pseudoknot.

The structure of SLI also differs from that of RNAI in that its stem is shorter by 4 bp and contains a small interior loop near its base (C575-A612), which in RNAI is closed by a G-U pairing (Fig. 4). To test whether these structural features of SLI are important for the formation or function of the pseudoknot, each was altered separately to make the lower stem of SLI resemble that of RNAI. Lengthening the stem of SLI (SLI+4) slightly reduced the expression of *repA* (1.6-fold) and the ability of RNAI to inhibit this expression, whereas removing the interior loop (C575U) had no significant effect on the expression or regulation of *repA* (Table 4). Therefore, the shorter stem and small interior loop of SLI are not significant factors in the formation or function of the pseudoknot. They are also unimportant for the binding of RNAI to SLI.

Thus, the structural requirements for the formation of pseudoknot are different from those for the binding between RNAI and SLI, again supporting the notion that the structural differences between SLI and RNAI are important in enabling SLI to participate efficiently in each of the two mutually exclusive reactions it is involved in.

Are there any other SLI structural requirements needed for pseudoknot formation? From the data presented above, it appears that efficient formation or function of the pseudoknot requires that the hairpin loop of SLI contains the five bases complementary to nt 703 to 707 of the distal pseudoknot sequence (with the bases G705, C706, and C707 being most important) and that a non-base-paired region be present directly below the hairpin loop. To determine whether there were other structural requirements for pseudoknot formation, the SLI of pMU720 was replaced by the SLI-equivalent structures from plasmids of the incompatibility groups $IncI_1$, IncZ, IncIγ, IncK, IncL/M, and IncFII (Fig. 6). The SLI-like structures from the four plasmids of the I-complex group (SLI.I_1, SLI.Z, SLI.Iγ, and SLI.K) were utilized because despite their different secondary structures, they all possess bases in their hairpin loops and upper stems which are complementary to all seven distal pseudoknot bases of pMU720 (Fig. 1). Furthermore, all members of the I-complex examined to date have the potential to form pseudoknots (i.e., possess complementary proximal and distal pseudoknot bases) and therefore should contain structures which are amenable to pseudoknot formation. The SLI-like structure from the IncL/M plasmid pMU604 (SLI.LM) was used because despite being only distantly related to I-complex plasmids, it has been shown to possess a regulatory system similar to that of IncB and $IncI_1$ plasmids (3). Thus, the expression of the Rep protein of pMU604 is dependent on the translation of a leader peptide and the formation of a pseudoknot, and both these events are negatively regulated by an antisense RNA. Although all data at present suggest that pseudoknot formation does not occur in IncFII plasmids, its SLI-like structure (SLI.FII) was used in this analysis because it contains exactly the same loop sequence as the IncB plasmid and therefore contains six bases complementary to the distal pseudoknot sequence of the IncB replicon.

To replace the IncB SLI with the analogous structures from the different plasmids, site-directed mutagenesis was used to create a unique *Xba*I site upstream of SLI (SLI.1 mutation) and a unique *Apa*I site within the 3′ lower stem of SLI (SLI.2 mutation [Fig. 4]). To avoid any complications arising from the expression of different chimeric RNAI molecules, the SLI.3 mutation (SLI.1 and SLI.2 mutations combined) was introduced into the *repA* fragment in which RNAI expression had been eliminated by the RNAI.3 mutation. The equivalent SLI regions from $IncI_1$, IncZ, IncIγ, IncK, IncFII, and IncL/M plasmids were amplified by PCR with forward and reverse primers containing *Xba*I and *Apa*I linkers, respectively, at their 5′ ends. These SLIs were then inserted into the *Xba*I-*Apa*I site, replacing the IncB SLI. The heterologous SLI structures were tested for their ability to form a functional pseudoknot in an IncB background by monitoring the level of *repA-lacZ* expression. To evaluate the ability of IncB RNAI to bind to these heterologous SLIs, assays were also performed in the presence of pMU617, a multicopy plasmid (20 to 30 copies per chromosome) carrying the wild-type IncB *rnaI* gene. Equivalent complementary antisense RNAI molecules, i.e., RNAI molecules containing the stem and loop structures of the heterologous plasmid but with the 5′ tail of the IncB plasmid were also constructed. The chimeric RNAI molecules were introduced in *trans* to *repA-lacZ* fusions carrying the different SLIs as a control to determine whether these SLI structures were able to fold correctly when introduced into an IncB plasmid background. Because the interaction between an antisense RNA and its target RNA is highly dependent on sequence and structural compatibility, only those chimeric SLI structures which are correctly folded should be able to interact with and be significantly affected by their corresponding chimeric RNAI molecules. Transcriptional fusions were also constructed to test for effects on transcription. In this experimental system, therefore, only the SLI has been changed; everything else which is required for pseudoknot formation in IncB plasmids, such as the leader peptide and distal pseudoknot sequence, remains unaltered.

Of the six different SLI-like structures used, only the ones from the non-I-complex plasmids IncL/M and IncFII did not contain in their hairpin loops and upper stems all seven of the bases that are complementary to the distal pseudoknot sequence of the IncB plasmid. To overcome this problem with the SLI.LM, the C residue at position 587 of this structure was deleted by site-directed mutagenesis (Fig. 6). The structure carrying this deletion (SLI.LMΔ) has six contiguous bases within its loop domain which are complementary to the distal pseudoknot sequence of the IncB plasmid. The mismatched seventh base (equivalent to position A598 in the IncB SLI) has been found to be unimportant for the formation of the pseudoknot in pMU720 (Table 2). The hairpin loop and upper stem of SLI.FII was also able to pair with only six of the possible seven pseudoknot bases. However, because the mismatched base (an A residue at position equivalent to G597 in IncB plasmids) was found to be important for the formation of

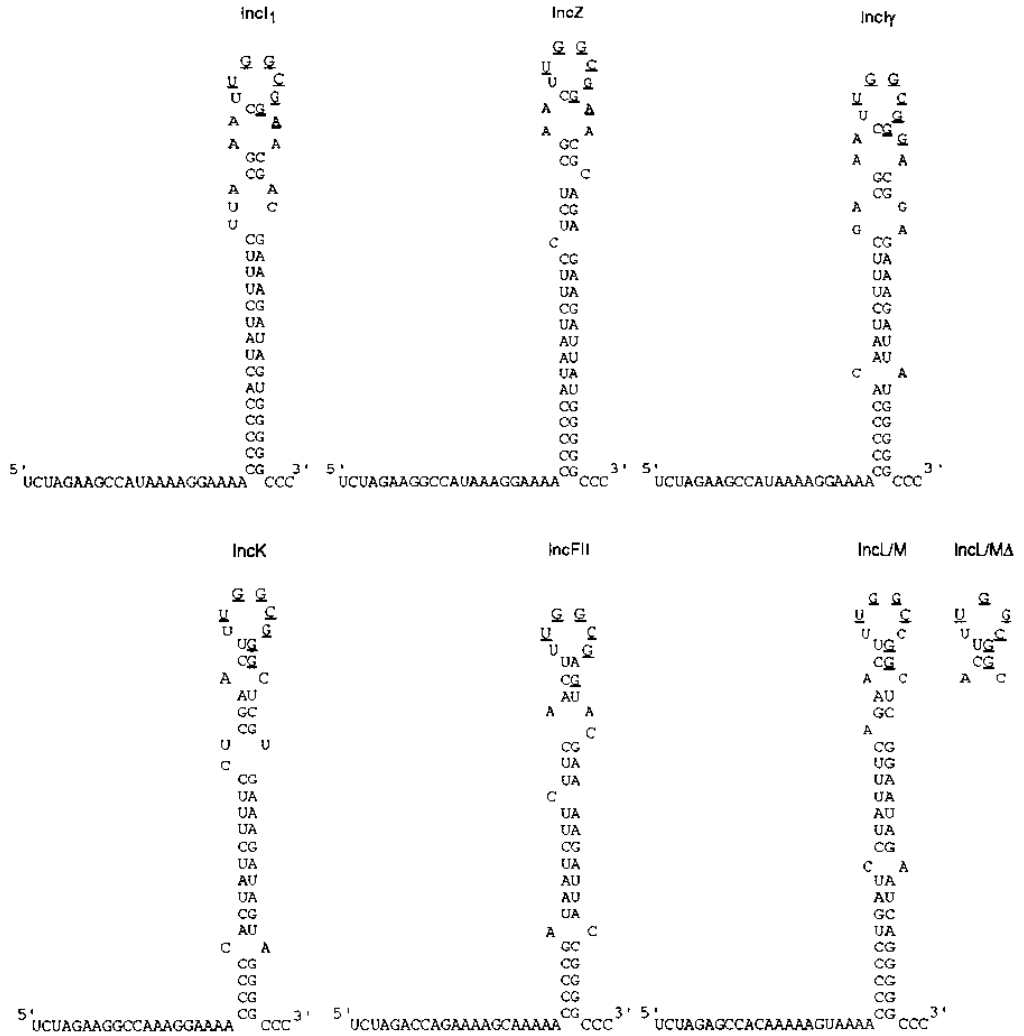

FIG. 6. Predicted secondary structures of the different SLI-like structures used to replace the IncB SLI. Bases in the loop of the SLI-like structures with the potential to base pair with the distal pseudoknot sequence of pMU720 are underlined. The IncFII SLI-like structure is based on a previous structural analysis, whereas the SLI-like structures from $IncI_1$, IncZ, and IncIγ are based on the structure of SLI obtained from pMU720. The structures of the other SLI-like structures are based purely on computer analysis.

the pseudoknot in pMU720 (Table 2) C703, the appropriate base in the distal pseudoknot sequence was changed to a U to allow possible A-U pairing at that position (SLI.FII+C703U mutation).

The results shown in Table 5 demonstrate that the introduction of the *Xba*I and *Apa*I sites (SLI.3) into the *repA-lacZ* fusions slightly reduced the β-galactosidase expression from both the translational (1.4-fold) and transcriptional (1.8-fold) fusions. Replacing the IncB SLI with $SLI.I_1$, SLI.Z, or SLI.Iγ increased expression from the *repA-lacZ* translational fusions 2.2-, 1.7-, and 1.3-fold, respectively, but also increased expression from the equivalent transcriptional fusions by approximately 2-fold. Substitution of SLI.K resulted in a slight decrease (1.5-fold) in β-galactosidase activity from the *repA-lacZ* translational fusion, despite a similar 2-fold increase in expression from the equivalent transcriptional fusion (Table 5).

As expected, replacement of the IncB SLI by the distantly related SLIs of SLI.FII, SLI.LM, or SLI.LMΔ resulted in severe reductions in *repA* expression. The introduction of the SLI.FII lowered expression from the translational *repA-lacZ* fusions by 202-fold (to 15 U) but from the transcriptional fusion by only 2-fold. Introduction of the C703U mutation (SLI.FII+A703U), which results in full complementarity between bases in the loop of SLI.FII and the distal pseudoknot sequence of IncB, increased β-galactosidase expression from the *repA-lacZ* translational fusion by 2-fold (33 U), but this was still 92-fold lower than seen with SLI.3 (Table 5). The transcriptional control indicates that this low level of expression is due to translational and not transcriptional effects. Furthermore, the complementary chimeric RNAI molecule was able to regulate the expression of the SLI.FII+A703U mutant (0.8 U) when introduced in *trans*, suggesting that the low level of expression was not due to incorrect folding of SLI.FII.

Similarly, introduction of SLI.LM lowered the expression of *repA* from the *repA-lacZ* translational fusion by 606-fold, and despite almost full complementarity between bases in the loop and the distal pseudoknot sequence of pMU720, expression of β-galactosidase from the SLI.LMΔ mutant was still 50-fold lower than that of SLI.3. Data obtained from the equivalent transcriptional controls show that the low level of *repA* expression from these mutants must result from inefficiencies in translational initiation (Table 5). As was the case with the

TABLE 5. Effect of replacing the IncB SLI with SLI equivalents of related plasmids on β-galactosidase expression from *repA-lacZ* fusions carrying the RNAI.3 mutation

Mutation	β-Galactosidase activity (U) from[a]:			
	Translational fusion with:			Transcriptional fusion with pBR322
	pBR322	pMU617 (RNAI)	Mutant RNAI[b]	
RNAI.3	4,130	0.2	NA[c]	991
SLI.3[d]	3,029	1.2	1.2	564
SLI.I[d]	6,619	40	0.4	1,357
SLI.Z[d]	5,280	5.6	0.8	1,237
SLI.Iγ[d]	3,973	1,142	0.7	1,256
SLI.K[d]	1,992	757	0.7	1,218
SLI.FII[d]	15	15	0.4	253
SLI.FII+A703U[d]	33	21	0.8	335
SLI.LM[d]	5.0	4.0	0.3	887
SLI.LMΔ[d]	61	58	0.6	1,625

[a] See Table 3, footnote *a*.
[b] The RNAI added in *trans* to fusions containing non-IncB SLIs was the appropriate chimeric RNAI molecule which retained full complementarity with the mutant RNAII target.
[c] NA, not applicable.
[d] The SLI mutations were present in *repA-lacZ* fusions carrying both the RNAI.3 and SLI.3 mutations.

SLI.FII, both SLI.LM and SLI.LMΔ appeared to fold correctly, since their complementary chimeric RNAI molecules significantly inhibited the expression of *repA-lacZ* (Table 5).

The expression of *repA* from the translational *lacZ* fusions containing the heterologous SLI-like structures was adequately controlled by their respective complementary antisense RNA molecules, whereas wild-type RNAI was able to significantly inhibit β-galactosidase expression only from the fusion carrying SLI.Z. These results mirror incompatibility experiments (22) which demonstrated that although plasmids belonging to the IncZ group were previously classified into a separate group from IncB plasmids, they are actually incompatible with IncB plasmids. These incompatibility data indicated that the IncZ antisense RNA is able to interact efficiently with the IncB RNAII and vice versa. The observation that the wild-type IncB RNAI could inhibit the expression of *repA* containing SLI.I_1 by 166-fold is also consistent with the incompatibility data, since incoming IncB plasmids displayed weak incompatibility against resident IncI_1 plasmids (18, 22).

The results of these SLI exchanges are largely consistent with the conclusions obtained from experiments investigating the effect of changing the secondary structure of SLI on the expression of *repA*. Thus, the formation and function of the pseudoknot in IncB plasmids appear to depend on both the complementarity between the proximal and distal pseudoknot bases and the presence of a non-base-paired region beneath the hairpin loop of SLI. The failure of the SLI.FII to permit the activation of the expression of *repA* can probably be attributed to its possessing the most stable upper stem region of all the SLI structures used in this study. The inability of the SLI.LMΔ to permit the formation of the pseudoknot is more difficult to explain since the stability of its upper stem is comparable to that of SLI.K. This finding may therefore indicate that the loop size of SLI and/or the position in the loop of the bases participating in the pseudoknot is also critical for the pseudoknot interaction or implicate other as-yet-unperceived differences between the two SLIs.

DISCUSSION

Physical analysis of the structure of SLI within the truncated molecule $RNAII_{107}$ confirmed that it differs from that of RNAI. First, the hairpin loop of SLI is proposed to exist in an equilibrium between a 4-base and a 6-base form, whereas the hairpin loop of RNAI is clearly a 6-base loop. Second, RNAI is proposed to contain nonconventional U-U base pairs immediately below the 6-base loop, whereas the existence of A-A mismatches in the comparable region of SLI results in the formation of a 4-base internal loop (the upper loop). In addition, the lower internal loop of SLI consists of 4 bases, whereas the corresponding internal loop in RNAI consists of only 2 bases.

Siemering et al. (27, 28) have previously elucidated the structural and sequence requirements for the interaction between RNAI and SLI. This interaction was proposed to consist of three major steps. The first one of these, the formation of the initial kissing complex, involves base pairing between complementary 3-base sequences located centrally in the hairpin loops of RNAI and SLI. In the second step, this initial complex prompts intrastrand melting and interstrand pairing of the upper stems of RNAI and SLI to produce the more stable extended kissing complex. The third step involves stabilization of the extended kissing complex by pairing between the complementary single-stranded tails of RNAI and SLI. In this model, the conversion of the initial kissing complex to the extended kissing complex is the key step in effective interaction between RNAI and RNAII and is facilitated by the presence of an interior loop in the upper stems of RNAI and SLI. The importance of such internal loops in interactions between antisense RNAs and their targets was subsequently confirmed by Hjalt and Wagner (11), who showed that the antisense RNA which regulates the copy number of the IncFII plasmid R1 also requires the presence of an internal loop in its upper stem for rapid binding to its target RNA and effective inhibitory activity.

Mutational analysis of the complementary pseudoknot sequences indicated that for the pseudoknot to form and efficiently enhance the expression of *repA* in pMU720, the presence of five pairs of complementary bases was required, these being the proximal nt 593 to 597 and the distal nt 703 to 707. However, mismatches between the other two pairs of complementary bases did affect the expression of *repA*, indicating that although not essential for the pseudoknot, they are involved in its formation or function. Increasing the extent of the complementarity between the two sequences did not significantly affect the expression of *repA* (Table 2), suggesting that the region of complementarity (7 bp) is optimal for the pseudoknot.

The results of the mutations in the proximal pseudoknot sequence are largely in agreement with those of Asano et al. (1), who found that base pairing at four specific matched positions is essential for pseudoknot formation. The discrepancy over the importance of the fifth pairing (between nt 597 and 703) can be attributed largely to the different mutations introduced at these positions, i.e., the nature of the mismatch in the pseudoknot, as well as the slight difference between the SLI structures of IncB and IncI_1 plasmids. Moreover, pairing between nt 597 and 703 appears to be less important for the formation of the pseudoknot in pMU720 than pairing between nt 593 to 596 and nt 704 to 707.

Investigation of the importance of SLI structure for the formation of an effective pseudoknot revealed that there was an absolute requirement for a non-base-paired region below the hairpin loop of SLI (upper interior loop), and even weak stabilization in this area by U-U base pairing (similar to that of RNAI) resulted in a 40-fold reduction in *repA* expression as

well as loss of sensitivity to regulation by RNAI (Table 4). The lower interior loop of SLI was not essential for the formation or function of the pseudoknot, since its complete closure (C584U-U585G) resulted in only a 1.5-fold reduction in *repA* expression. This is in contrast to the RNAI-SLI interaction which requires the presence of this interior loop and the corresponding interior loop in RNAI to facilitate formation of the extended kissing complex. These results indicate that the mechanism of binding of SLI to the distal pseudoknot bases is fundamentally different from that of SLI to RNAI, supporting the notion that the structural difference between RNAI and SLI endows SLI with the ability to participate efficiently in these two competing binding reactions.

Replacement of the SLI of pMU720 by similar SLI-like structures from $IncI_1$, IncZ, IncIγ, and IncK plasmids did not significantly inhibit the expression of *repA*, reinforcing the belief that pseudoknot formation occurs in all I-complex plasmids. Since these SLI-like structures are most different in the conformation and the sequences of their lower stems, it indicates that as long as the stem is relatively stable, this region is not important for the formation or function of the pseudoknot. The data obtained with the different I-complex SLIs are generally in agreement with the results obtained with the mutants of the SLI of IncB (Table 4) in that they suggest that an SLI-like structure need only have proximal pseudoknot bases located in a 4- or 6-base hairpin loop, and an incompletely paired region immediately below this loop, for it to be able to participate in the formation of a functional pseudoknot. SLI.FII+A703U, one of the two SLIs which formed the pseudoknot inefficiently, although satisfying the first criterion, contains extensive pairing below the loop domain which may inhibit the pseudoknot interaction. However, stabilization of the upper stem does not account for the extremely low level of expression of *repA* with the SLI.LMΔ, suggesting that other factors such as the size of the SLI loop or the position of the proximal pseudoknot bases within this loop may be important for efficient formation of the pseudoknot. This notion is supported by data showing that when C587 of SLI.LM is replaced by a G so that the hairpin loop of SLI.LM becomes identical to that of the other SLIs tested here, the level of *repA* expression is approximately 16-fold higher than that seen with SLI.LMΔ, the mutant in which C587 had been deleted (4).

The data obtained from swapping the SLI of IncB with the SLI-like structures of other I-complex plasmids indicate that the pseudoknot interaction (between SLI and the distal pseudoknot sequence) possesses only limited specificity, relying mainly on the complementarity of the proximal and distal pseudoknot sequences in conjunction with an incompletely paired region below the hairpin loop of SLI. By contrast, the RNAI-SLI interaction is highly specific, as demonstrated when wild-type IncB RNAI was added in *trans* to *repA-lacZ* fusions carrying the different SLI-like structures. Thus, apart from SLI.Z, wild-type RNAI could not efficiently control the expression of *repA* from *repA-lacZ* fusions containing any of the other I-complex SLI structures, even though these SLI-like structures have similar loop sequences. These data are consistent with the model for binding between RNAI and SLI which states that complementarity in the hairpin loops as well as the structure and identity of the lower interior loop are factors critical for an effective binding reaction. The reason that the IncB system has evolved distinct mechanisms with different specificities of binding for the two RNA interactions involving SLI probably reflects the biological functions and locations of the molecules participating in these interactions. Since the cellular concentration of free RNAI is a critical parameter in the modulation of *repA* expression, it is important that RNAI interacts stably only with its intended target, SLI, and does not become sequestered in nonspecific associations with cellular RNAs. The key to the fulfillment of this requirement is the folding of RNAI and SLI into stem-loop structures, which facilitates their participation in a highly specific binding reaction (27, 28). The critical step in this binding reaction is the intrastrand melting reaction that converts the transient initial kissing complex between RNAI and SLI to the more stable extended kissing complex. This reaction is made possible by the lower interior loops present in RNAI and SLI and is presumably triggered by the interaction between their complementary hairpin loops. Thus, RNAI is able to interact transiently with cellular RNAs but only progresses to a more stable interaction when it encounters its appropriate target. After disruption of SLIII, the distal pseudoknot sequence is predicted to exist within a linear region of RNA. The data presented here suggest that the interaction between the hairpin loop of SLI and the distal pseudoknot sequence is not sufficient to act as a trigger for melting of an even moderately stable upper stem (UU and stable-pairing SLI upper-stem mutants). Therefore, it appears that the structural differences between SLI and RNAI have evolved because of the need to weaken the upper stem of SLI to facilitate efficient formation of the pseudoknot, without weakening the upper stem of RNAI to the point of compromising its specificity of binding. One consequence of this may have been a decrease in specificity of the pseudoknot binding reaction, which requires only five bases of continuous complementarity between the loop of SLI and a linear region of RNA to form a relatively stable interaction (SLI swap data). However, this potential problem is ameliorated by the fact that SLI does not need to scan through cellular RNAs to find its target. That is, if SLI is not bound to RNAI, then its alternative target, the distal pseudoknot sequence, can be found on the same RNA molecule. Therefore, the IncB system provides us with a clear example of the evolutionary manipulation of secondary structure to produce RNAs that, although complementary, have distinct binding specificities in line with their different biological functions.

The structural difference between the antisense RNA and its target RNA (Fig. 4) appears to be an important feature of the RNA molecules involved in the regulation of initiation of replication of group B and other I-complex plasmids. This is the first example of modulation of the binding activities of complementary RNAs by the manipulation of their secondary structure and may be unique to pseudoknot-forming plasmids. Since the kinetics of the interaction of only a few antisense RNA-target RNA systems are known and there is presently no information on the kinetics of the pseudoknot interaction in I-complex and IncL/M plasmids, it is impossible to ascertain the extent to which their structural differences affect the efficiency of pseudoknot and antisense-target RNA interactions. However, the apparent second-order rate constant of the RNAI-SLI binding reaction in pMU720 calculated by Siemering et al. (28) to be $7.6 \times 10^5\ M^{-1}\ s^{-1}$ closely correlates with the values of 7.1×10^5 and $1 \times 10^6\ M^{-1}\ s^{-1}$ obtained for the antisense RNA-target RNA binding in the ColE1 and IncFII systems, respectively (19, 31), and all are close to the association rate for the nucleation of base pairing (6, 20). This indicates that the structural differences between antisense and target RNAs do not impair their ability to hybridize efficiently.

ACKNOWLEDGMENTS

This work was supported by a grant from the National Health and Medical Research Council. I. W. Wilson and K. R. Siemering were each a recipient of an Australian Postgraduate Research Award.

We thank Jing Hong An and Jiang Yan for excellent technical assistance.

REFERENCES

1. **Asano, K., A. Kato, H. Moriwaki, C. Hama, K. Shiba, and K. Mizobuchi.** 1991. Positive and negative regulations of plasmid ColIb-P9 *repZ* gene expression at the translational level. J. Biol. Chem. **266:**3774–3781.
2. **Asano, K., H. Moriwaki, and K. Mizobuchi.** 1991. An induced mRNA secondary structure enhances *repZ* translation in plasmid ColIb-P9. J. Biol. Chem. **266:**24549–24556.
3. **Athanasopoulos, V., J. Praszkier, and A. J. Pittard.** 1995. The replication of an IncL/M plasmid is subject to antisense control. J. Bacteriol. **177:**4730–4741.
4. **Athanasopoulos, V., J. Praszkier, and A. J. Pittard.** 1996. Unpublished data.
5. **Bird, P. I., and J. Pittard.** 1983. Demonstration of a third incompatibility function on plasmids already incompatible with group P and group I plasmids. Plasmid **9:**191–200.
6. **Craig, M. E., D. M. Crothers, and P. Doty.** 1971. Relaxation kinetics of dimer formation by self complementary oligonucleotides. J. Mol. Biol. **62:**383–401.
7. **Davey, R. B. D., P. I. Bird, S. M. Nikoletti, J. Praszkier, and J. Pittard.** 1984. The use of mini-Gal plasmids for the rapid incompatibility grouping of conjugative R plasmids. Plasmid **11:**234–242.
8. **Gil, D., and J.-P. Bouché.** 1991. ColE1-type vectors with fully repressible replication. Gene **105:**17–22.
9. **Groebe, D. R., and O. C. Uhlenbeck.** 1988. Characterization of RNA hairpin loop stability. Nucleic Acids Res. **16:**11725–11735.
10. **Hjalt, T., and E. G. H. Wagner.** 1992. The effect of loop size in antisense and target RNAs on the efficiency of antisense RNA control. Nucleic Acids Res. **20:**6723–6732.
11. **Hjalt, T. H., and E. G. H. Wagner.** 1995. Bulged-out nucleotides in an antisense RNA are required for rapid target RNA binding *in vitro* and inhibition *in vivo*. Nucleic Acids Res. **23:**580–587.
12. **Jaeger, J. A., D. H. Turner, and M. Zuker.** 1989. Improved predictions of secondary structures for RNA. Proc. Natl. Acad. Sci. USA **86:**7706–7710.
13. **Jaeger, J. A., D. H. Turner, and M. Zuker.** 1990. Predicting optimal and suboptimal secondary structures for RNA. Methods Enzymol. **183:**281–306.
14. **Kieny, M. P., R. Lathe, and J. P. Lecocq.** 1983. New versatile cloning and sequencing vectors based on bacteriophage M13. Gene **26:**91–99.
15. **Messing, J.** 1983. New M13 vectors for cloning. Methods Enzymol. **101:**20–78.
16. **Miller, J. H.** 1972. Experiments in molecular genetics, p. 352–355. Cold Spring Harbor Laboratory, Cold Spring Harbor, N.Y.
17. **Monod, J., G. Cohen-Bazire, and M. Cohen.** 1951. Sur la biosynthése de la β-galactosidase (lactase) chez *Escherichia coli*. La specificité de l'induction. Biochim Biophys. Acta **7:**585–599.
18. **Nikoletti, S., P. Bird, J. Praszkier, and J. Pittard.** 1988. Analysis of the incompatibility determinants of I-complex plasmids. J. Bacteriol. **170:**1311–1318.
19. **Persson, C., E. G. H. Wagner, and K. Nordström.** 1988. Control of replication of plasmid R1: kinetics of *in vitro* interaction between the antisense RNA, CopA, and its target, CopT. EMBO J. **7:**3279–3288.
20. **Pörschke, D., and M. Eigen.** 1971. Co-operative non-enzymic base recognition. III. Kinetics of the helix-coil transition of the oligoribouridylic · oligoriboadenylic acid system and of oligoriboadenylic acid alone at acidic pH. J. Mol. Biol. **62:**361–381.
21. **Praszkier, J., P. Bird, S. Nikoletti, and A. J. Pittard.** 1989. Role of countertranscript RNA in the copy number control system of an IncB miniplasmid. J. Bacteriol. **171:**5056–5064.
22. **Praszkier, J., P. Bird, K. Siemering, and J. Pittard.** 1991. Comparative analysis of the replication regions of the IncB, IncK, and IncZ plasmids. J. Bacteriol. **173:**2393–2397.
23. **Praszkier, J., I. W. Wilson, and A. J. Pittard.** 1992. Mutations affecting translational coupling between the *rep* genes of an IncB miniplasmid. J. Bacteriol. **174:**2376–2383.
24. **Sambrook, J., E. F. Fritsch, and T. Maniatis.** 1989. Molecular cloning: a laboratory manual, 2nd ed. Cold Spring Harbor Laboratory, Cold Spring Harbor, N.Y.
25. **Sanger, F., S. Nicklen, and A. R. Coulson.** 1977. DNA sequencing with chain-terminating inhibitors. Proc. Natl. Acad. Sci. USA **74:**5463–5467.
26. **Santa Lucia, J., Jr., R. Kierzek, and D. H. Turner.** 1991. Stabilities of consecutive A · C, C · C, G · G, U · C, and U · U mismatches in RNA internal loops: evidence for stable hydrogen-bonded U · U and C · C+ pairs. Biochemistry **30:**8242–8251.
27. **Siemering, K. R., J. Praszkier, and A. J. Pittard.** 1993. Interaction between the antisense and target RNAs involved in the regulation of IncB plasmid replication. J. Bacteriol. **175:**2895–2906.
28. **Siemering, K. R., J. Praszkier, and A. J. Pittard.** 1994. Mechanism of binding of the antisense and target RNAs involved in the regulation of the IncB plasmid replication. J. Bacteriol. **176:**2677–2688.
29. **Sutcliffe, J. G.** 1979. Complete nucleotide sequence of the *Escherichia coli* plasmid pBR322. Cold Spring Harbor Symp. Quant. Biol. **43:**77–90.
30. **Tinoco, I., P. N. Borer, B. Dengler, M. D. Levine, O. C. Uhlenbeck, D. M. Crothers, and J. Gralla.** 1973. Improved estimation of secondary structure in ribonucleic acids. Nature (London) New Biol. **246:**40–41.
31. **Tomizawa, J.** 1984. Control of ColE1 plasmid replication: the process of binding of RNA I to the primer transcript. Cell **38:**861–870.
32. **Vandeyar, M. A., M. P. Weiner, C. J. Hutton, and C. A. Batt.** 1988. A simple and rapid method for the selection of oligodeoxynucleotide-directed mutants. Gene **65:**129–133.
33. **Wagner, E. G. H., and K. Nordström.** 1986. Structural analysis of an RNA molecule involved in replication control of plasmid R1. Nucleic Acids Res. **14:**2523–2538.
34. **Wilson, I. W.** 1995. Molecular analysis of the replication control system of IncB plasmids. Ph.D. thesis. The University of Melbourne, Parkville, Australia.
35. **Wilson, I. W., P. J., and A. J. Pittard.** 1993. Mutations affecting pseudoknot control of the replication of B group plasmids. J. Bacteriol. **175:**6476–6483.
36. **Wilson, I. W., J. Praszkier, and A. J. Pittard.** 1994. Molecular analysis of RNAI control of *repB* translation in IncB plasmids. J. Bacteriol. **176:**6497–6508.
37. **Wrede, P., R. Wurst, J. Vournakis, and A. Rich.** 1979. Conformational changes of yeast $tRNA^{Phe}$ and *E. coli* $tRNA_2^{Glu}$ as indicated by different nuclease digestion patterns. J. Biol. Chem. **254:**9608–9616.
38. **Yang, J., S. Ganesan, J. Sarsero, and A. J. Pittard.** 1993. A genetic analysis of various functions of the TyrR protein of *Escherichia coli*. J. Bacteriol. **175:**1767–1776.
39. **Zuker, M.** 1989. On finding all suboptimal foldings of an RNA molecule. Science **244:**48–52.